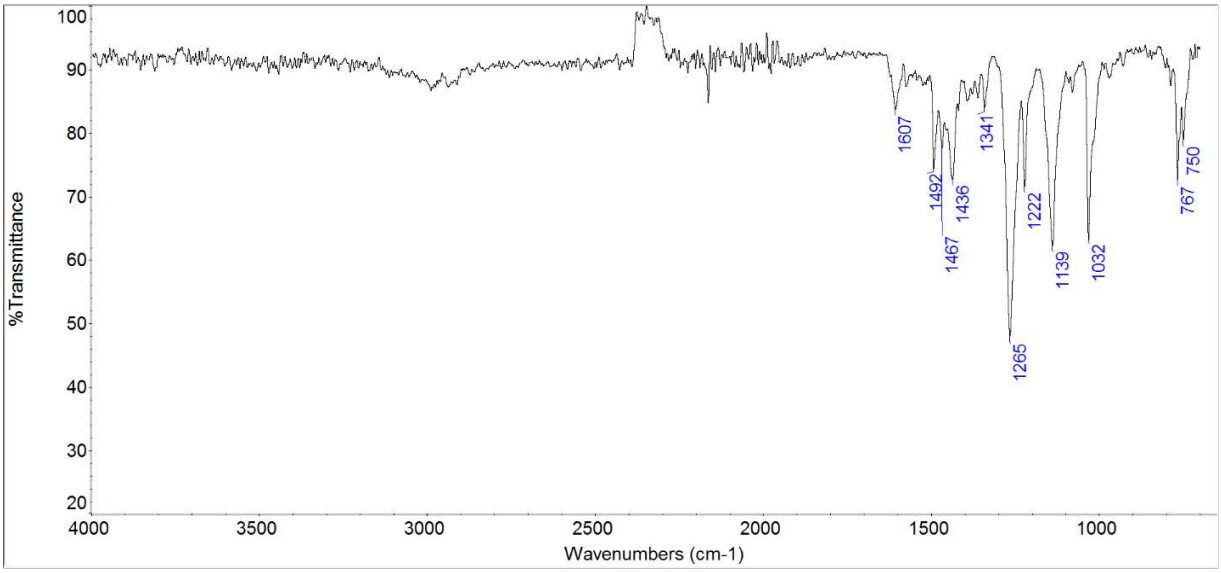

a)

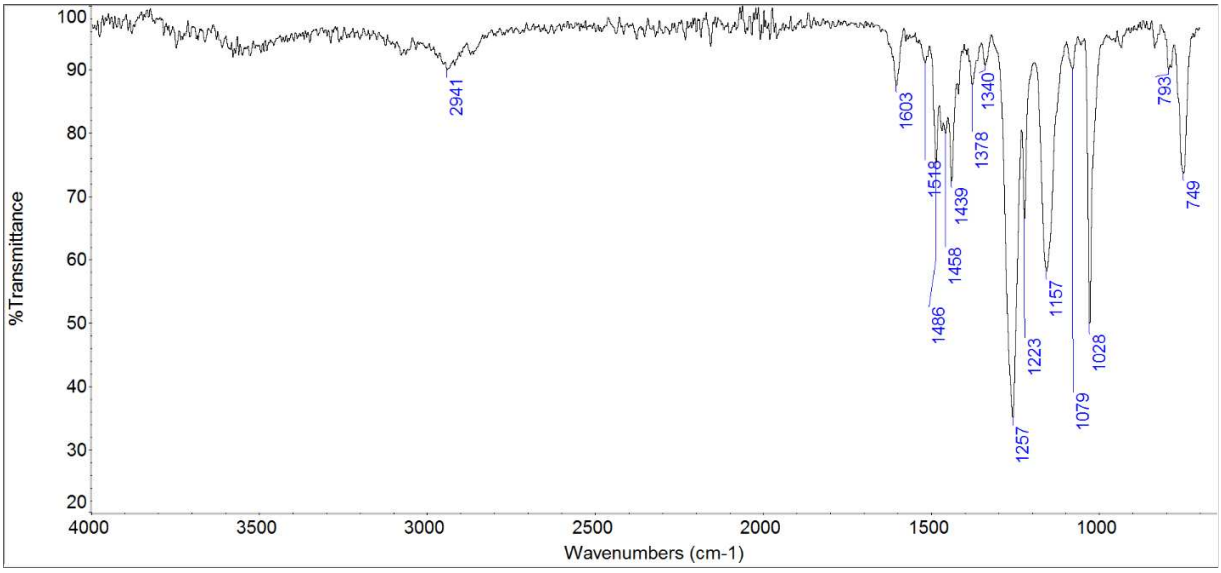

b)

Fig. S1 AT IR spectra of a) **1**, and b) **2**.

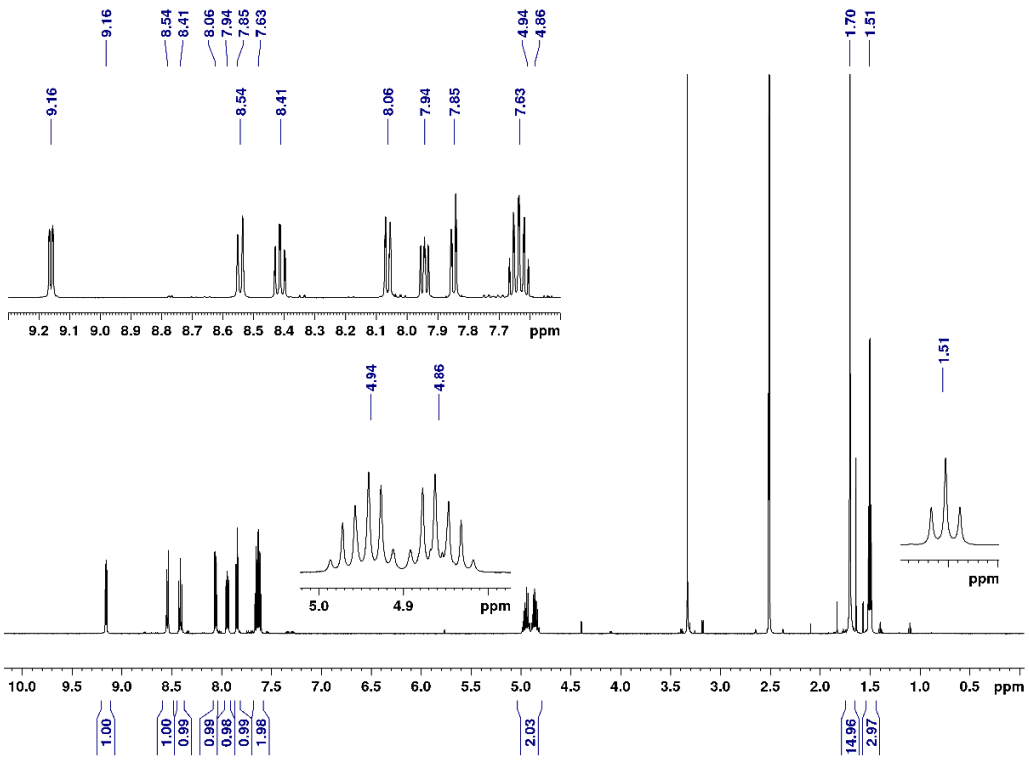
9.16
8.54
8.41
8.06
7.94
7.85
7.63
4.94
4.86
1.70
1.51
ppm
1.00
0.99
0.98
2.03
14.96
2.97

a)

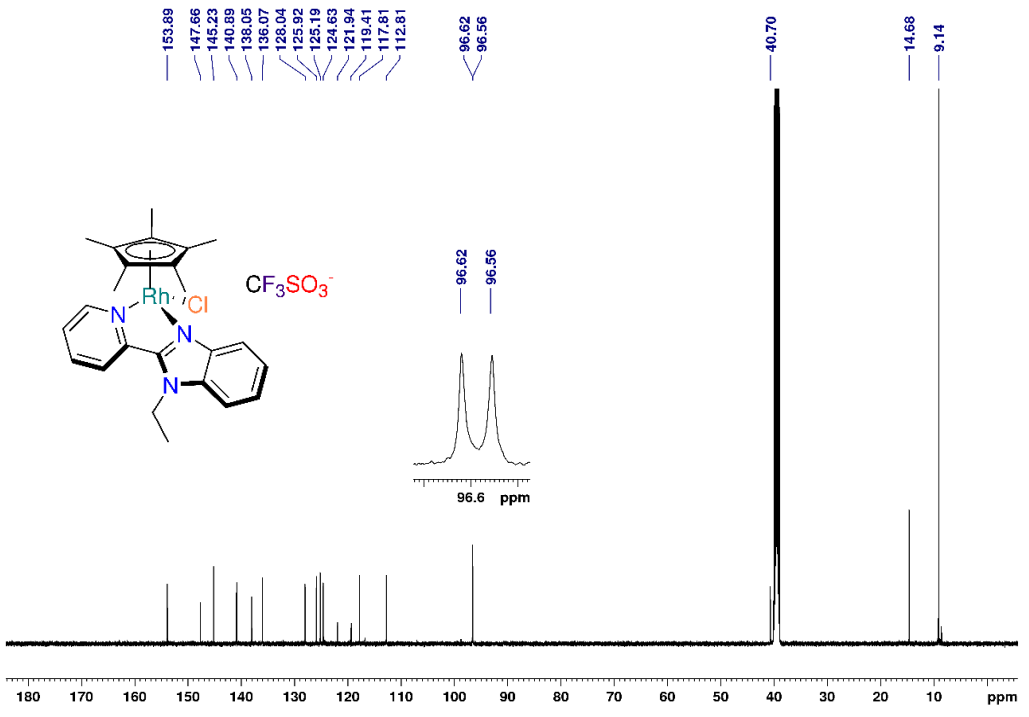
153.89
147.66
145.23
140.89
138.05
136.07
128.04
125.92
125.19
124.63
121.94
119.41
117.81
112.81
96.62
96.56
40.70
14.68
9.14
Rh
Cl
N
N
N
CF3SO3-
ppm

b)

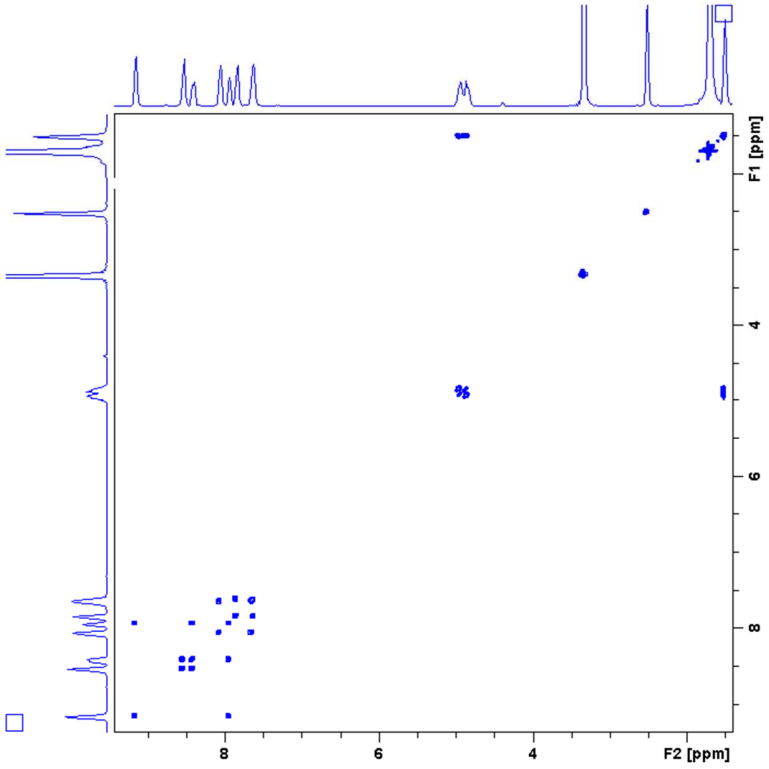

c)

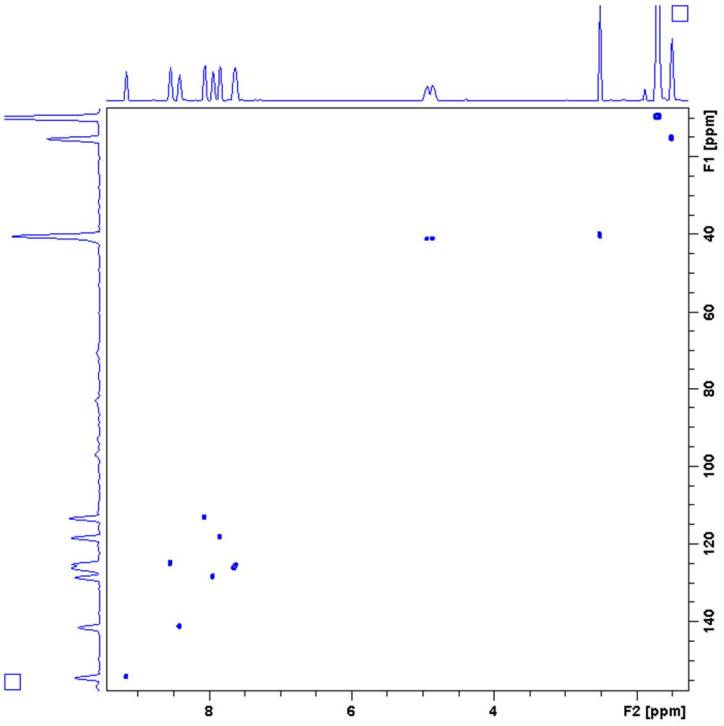

d)

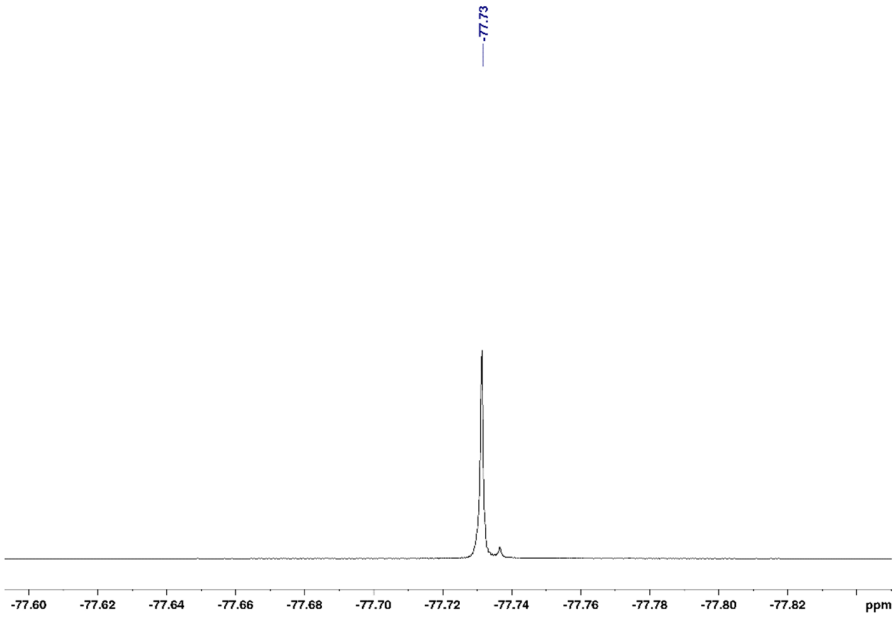

e)

Fig. S2 NMR analysis of **1** in DMSO-d_6, a) ^{1}H, b) ^{13}C, c) {^{1}H, ^{1}H} COS90, d) {^{13}C, ^{1}H} HSQC and e) ^{19}F.

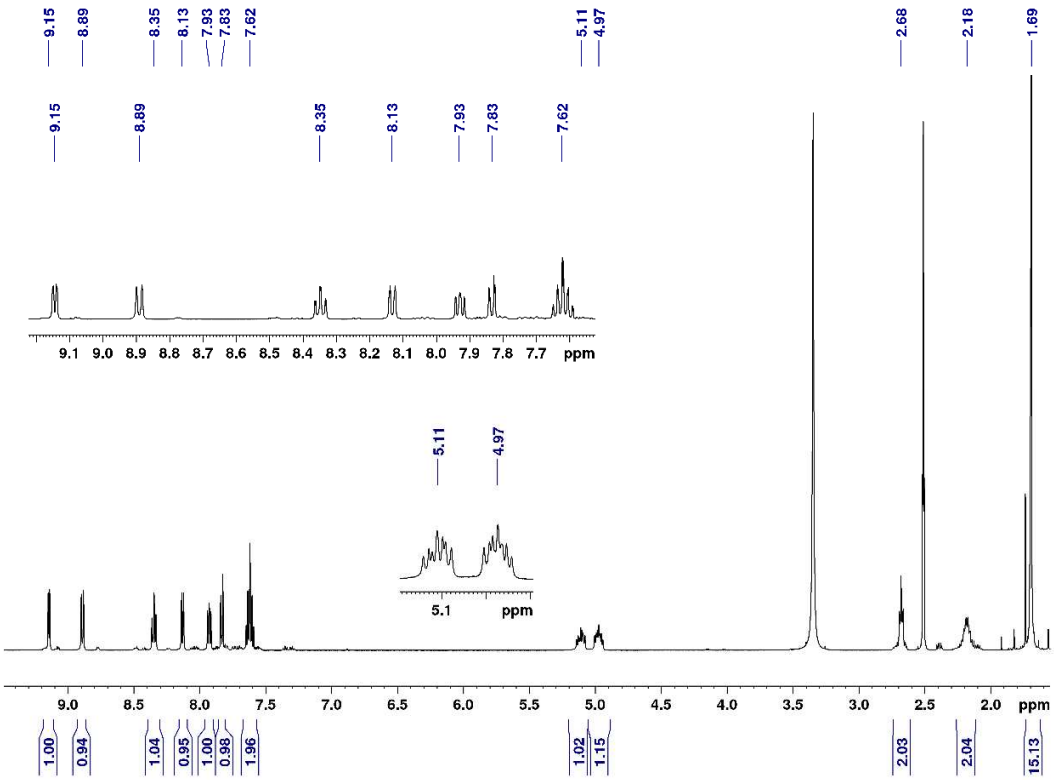
9.15
8.89
8.35
8.13
7.93
7.83
7.62
5.11
4.97
2.68
2.18
1.69
9.1 9.0 8.9 8.8 8.7 8.6 8.5 8.4 8.3 8.2 8.1 8.0 7.9 7.8 7.7 ppm
5.1 ppm
9.0 8.5 8.0 7.5 7.0 6.5 6.0 5.5 5.0 4.5 4.0 3.5 3.0 2.5 2.0 ppm
1.00 0.94 1.04 0.95 1.00 0.98 1.96 1.02 1.15 2.03 2.04 15.13

a)

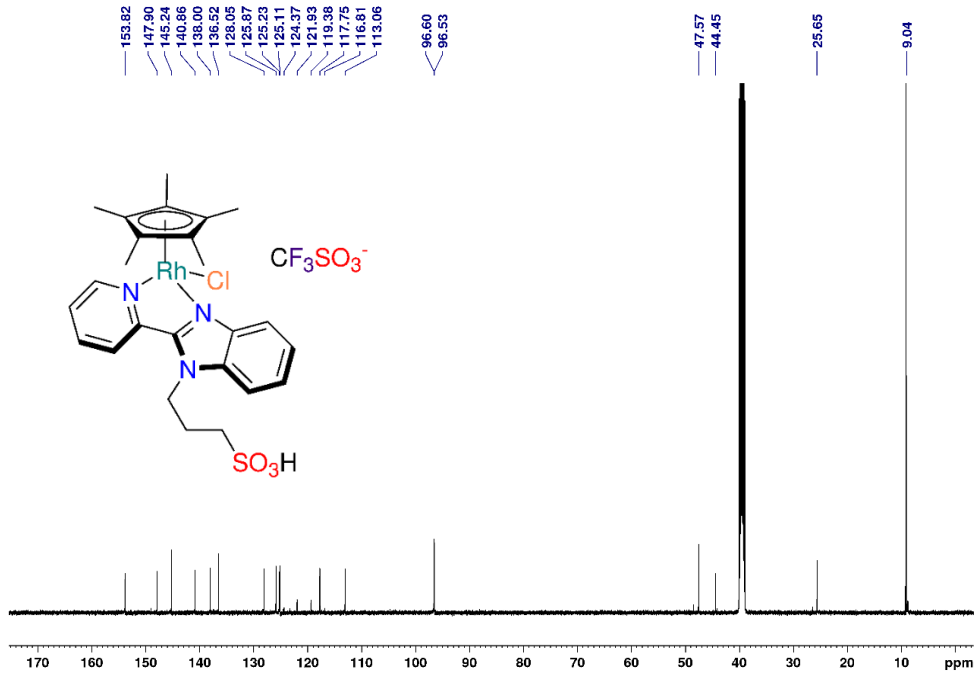
153.82
147.90
145.24
140.86
138.00
136.52
128.05
125.87
125.23
125.11
124.37
121.93
119.38
117.75
116.81
113.06
96.60
96.53
47.57
44.45
25.65
9.04
Rh
Cl
N
N
N
CF3SO3-
SO3H
170 160 150 140 130 120 110 100 90 80 70 60 50 40 30 20 10 ppm

b)

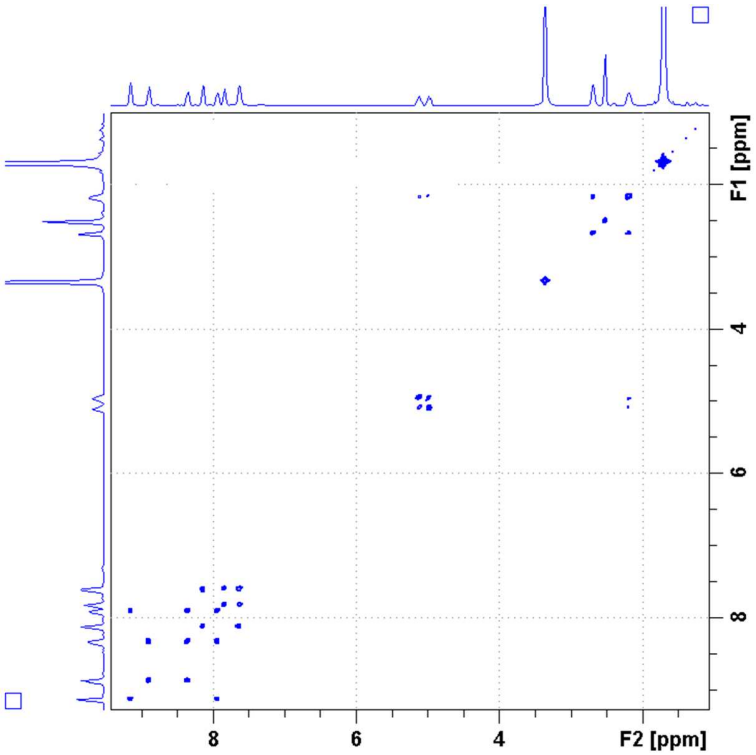

c)

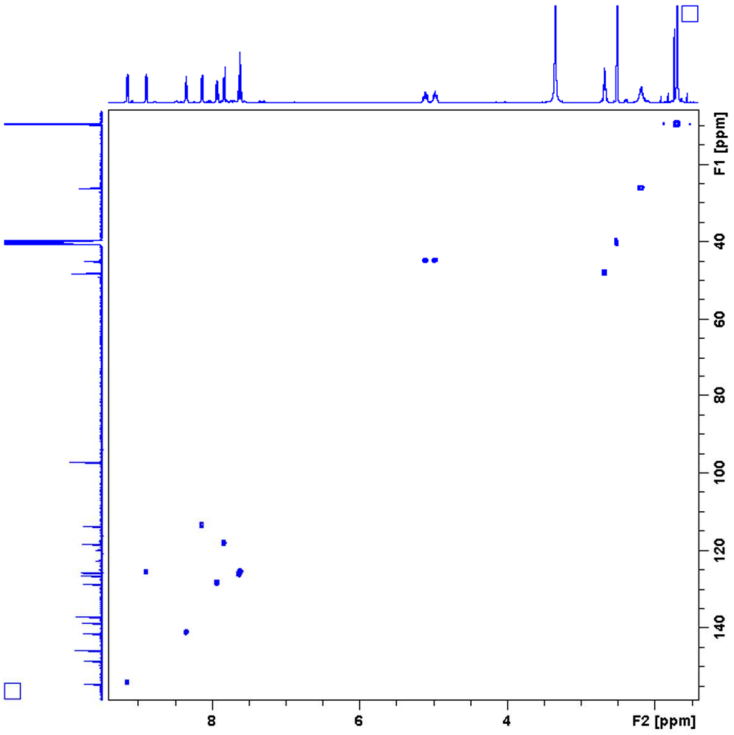

d)

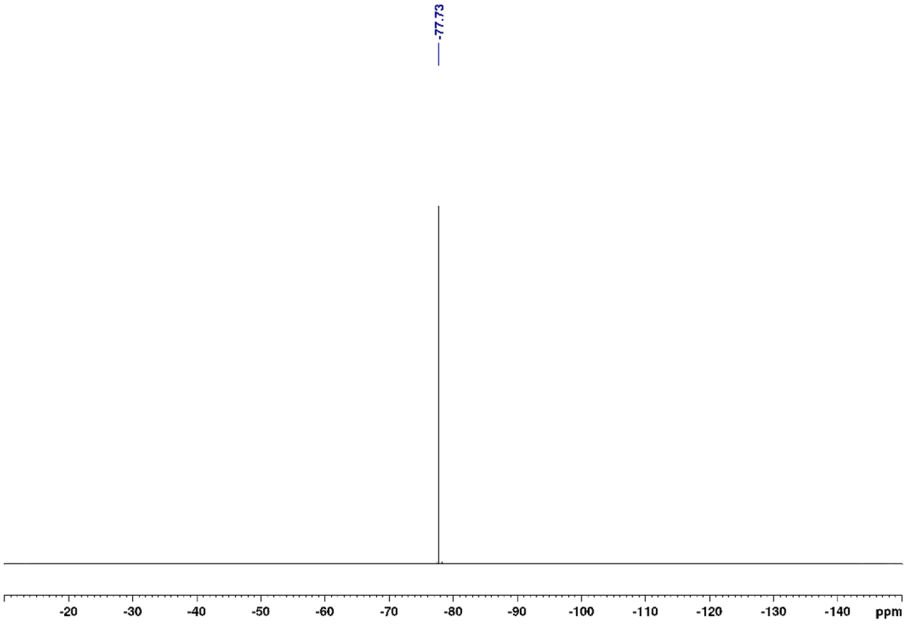

e)

Fig. S3 NMR analysis of **2** in DMSO-d_6, a) ^{1}H, b) ^{13}C, c) {^{1}H, ^{1}H} COS90, d) {^{13}C, ^{1}H} HSQC and e) ^{19}F.

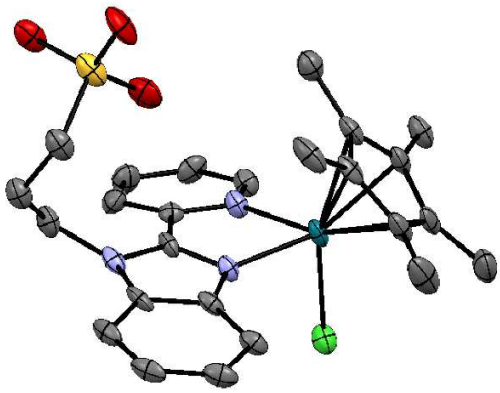

Fig. S4 Molecular structure of **2** (thermal ellipsoids are shown at 50 % probability level). Hydrogen atoms were omitted for the clarity.

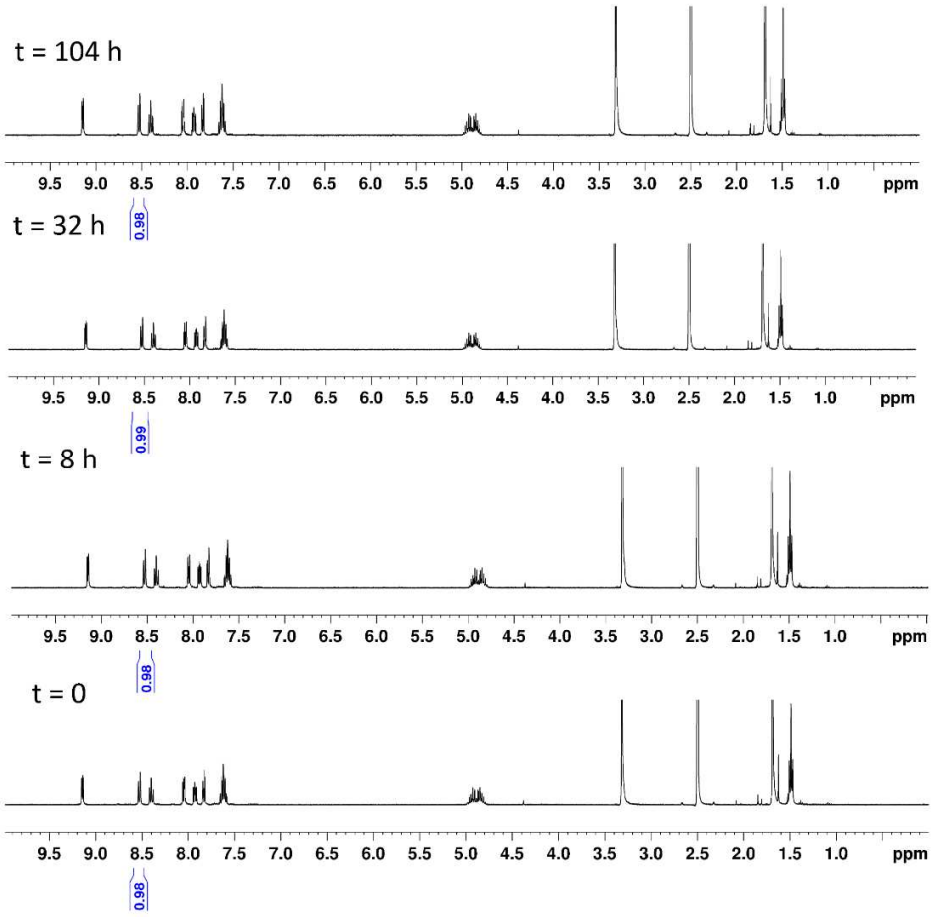
t = 104 h
9.5 9.0 8.5 8.0 7.5 7.0 6.5 6.0 5.5 5.0 4.5 4.0 3.5 3.0 2.5 2.0 1.5 1.0 ppm
0.98
t = 32 h
9.5 9.0 8.5 8.0 7.5 7.0 6.5 6.0 5.5 5.0 4.5 4.0 3.5 3.0 2.5 2.0 1.5 1.0 ppm
0.99
t = 8 h
9.5 9.0 8.5 8.0 7.5 7.0 6.5 6.0 5.5 5.0 4.5 4.0 3.5 3.0 2.5 2.0 1.5 1.0 ppm
0.96
t = 0
9.5 9.0 8.5 8.0 7.5 7.0 6.5 6.0 5.5 5.0 4.5 4.0 3.5 3.0 2.5 2.0 1.5 1.0 ppm
0.98

a)

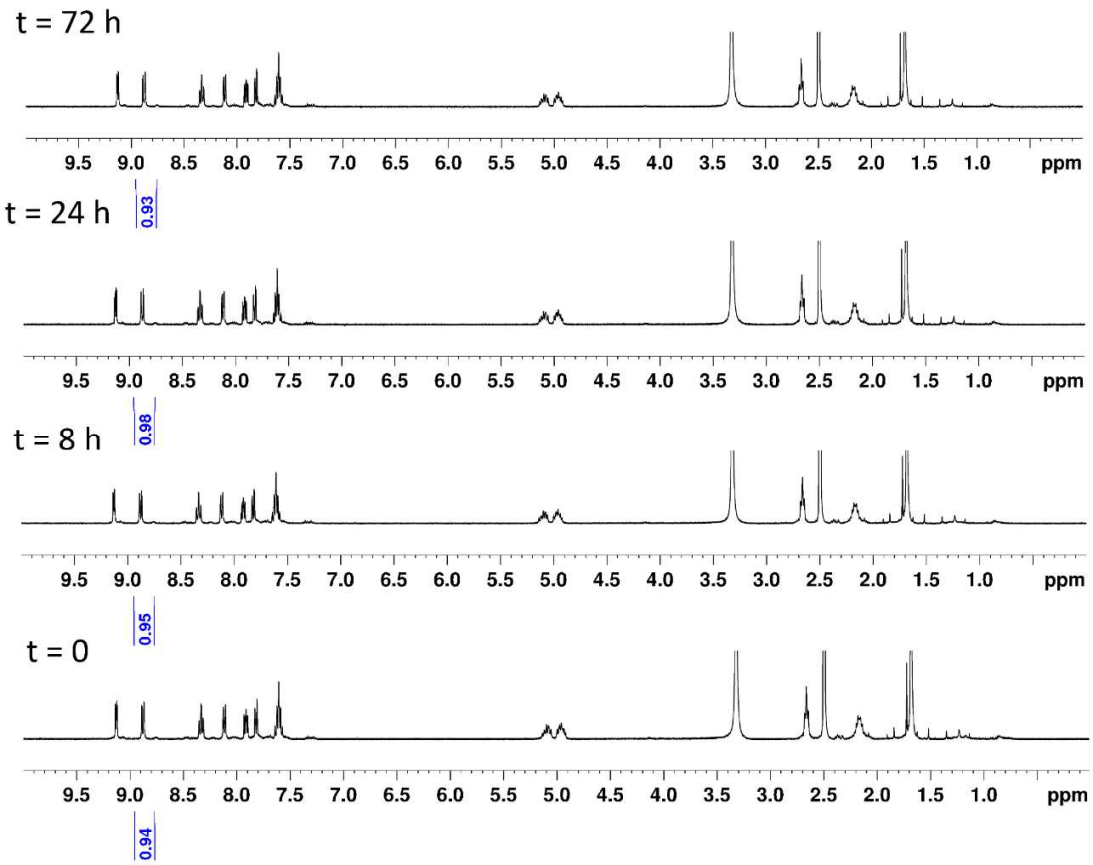

b)

Fig. S5 Stability of a) **1** and b) **2** in DMSO-d_6 followed by ^{1}H NMR at different time interval.

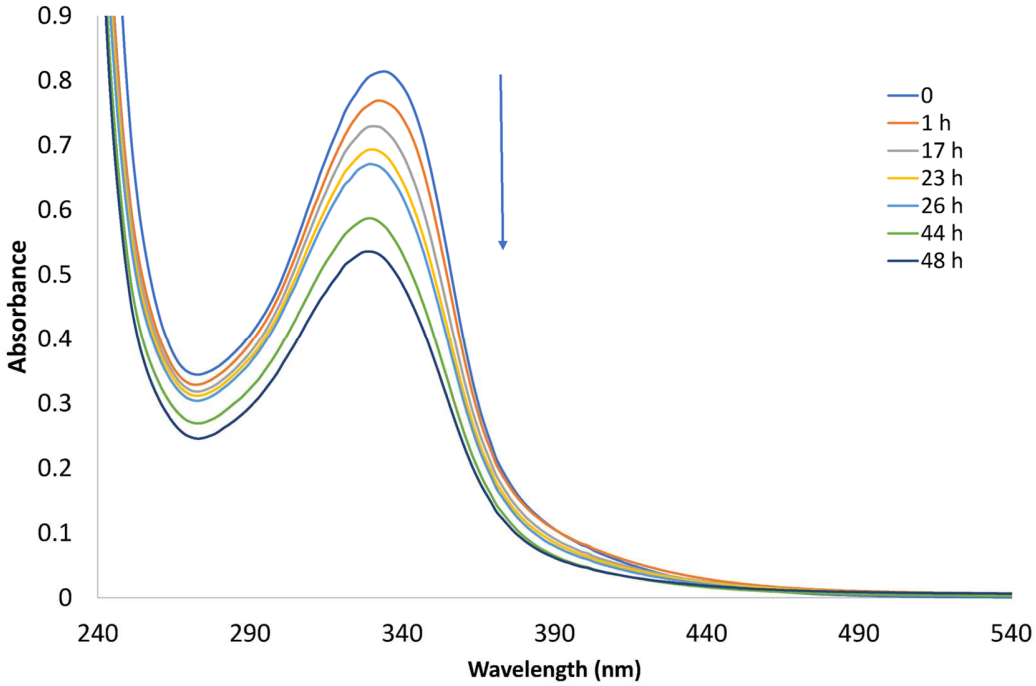
0.9
0.8
0.7
0.6
0.5
0.4
0.3
0.2
0.1
0
Absorbance
240
290
340
390
440
490
540
Wavelength (nm)
0
1 h
17 h
23 h
26 h
44 h
48 h

a)

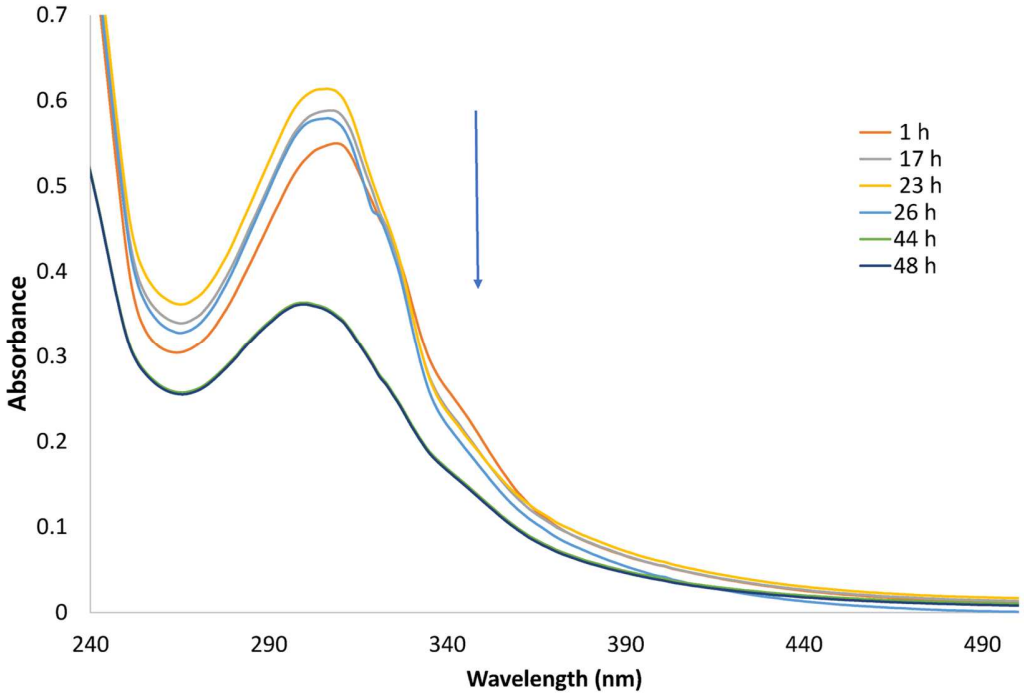
0.7
0.6
0.5
0.4
0.3
0.2
0.1
0
Absorbance
240
290
340
390
440
490
Wavelength (nm)
1 h
17 h
23 h
26 h
44 h
48 h

b)

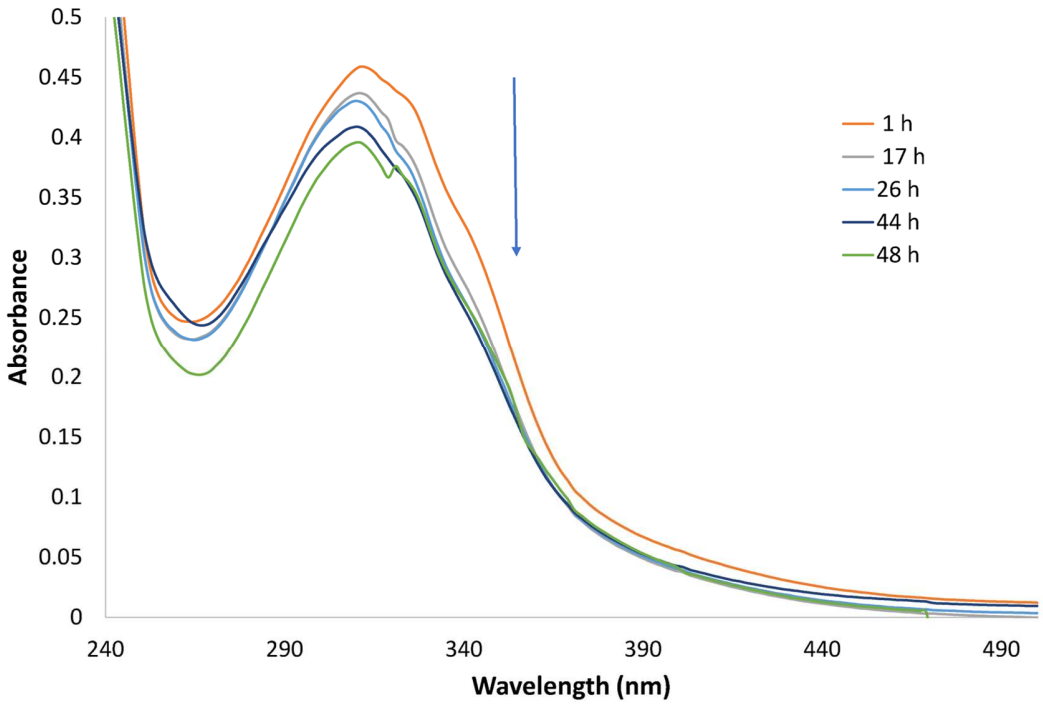
0.5
0.45
0.4
0.35
0.3
0.25
0.2
0.15
0.1
0.05
0
Absorbance
240
290
340
390
440
490
Wavelength (nm)
1 h
17 h
26 h
44 h
48 h

c)

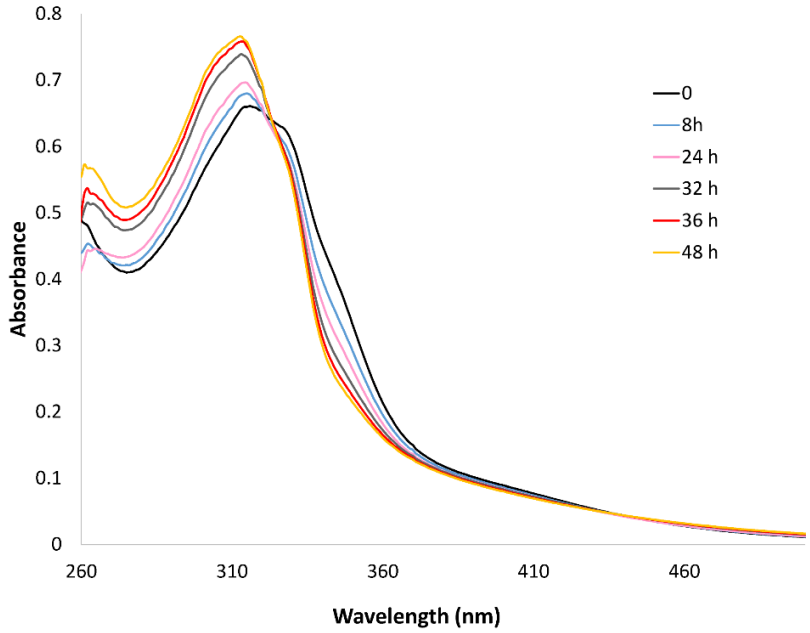
0.8
0.7
0.6
0.5
0.4
0.3
0.2
0.1
0
Absorbance
260
310
360
410
460
Wavelength (nm)
0
8h
24 h
32 h
36 h
48 h

d)

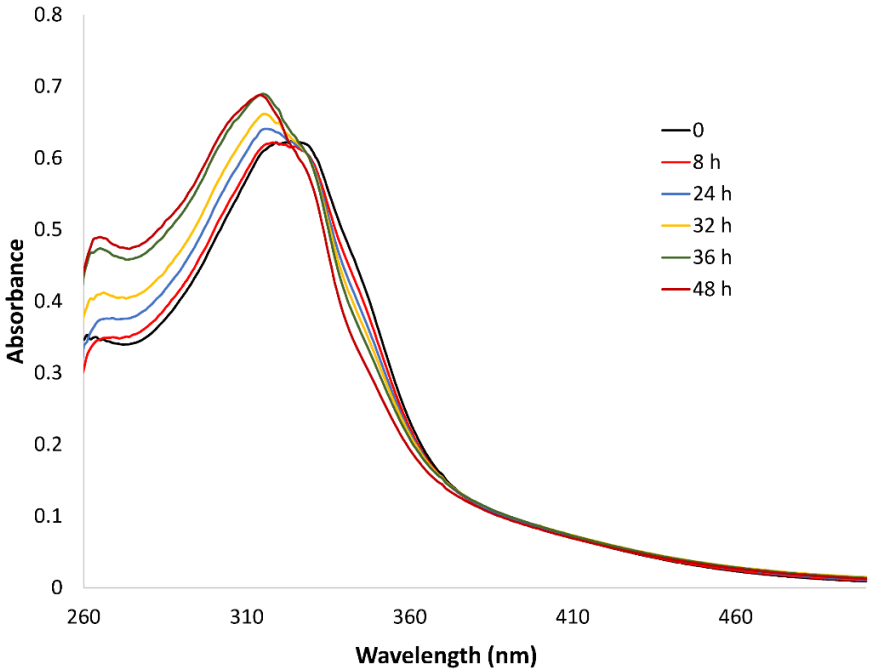

e)

Fig. S6 UV-Vis spectra of a) **1** (20% (v/v) DMSO/PBS (0.1 M)), b) **2** (0.1 M PBS) and c) **2** (20% (v/v) methanol/PBS (0.1 M)), d) **1** (DMSO) and e) **2** (DMSO) recorded as a function of time during the incubation for 48 h.

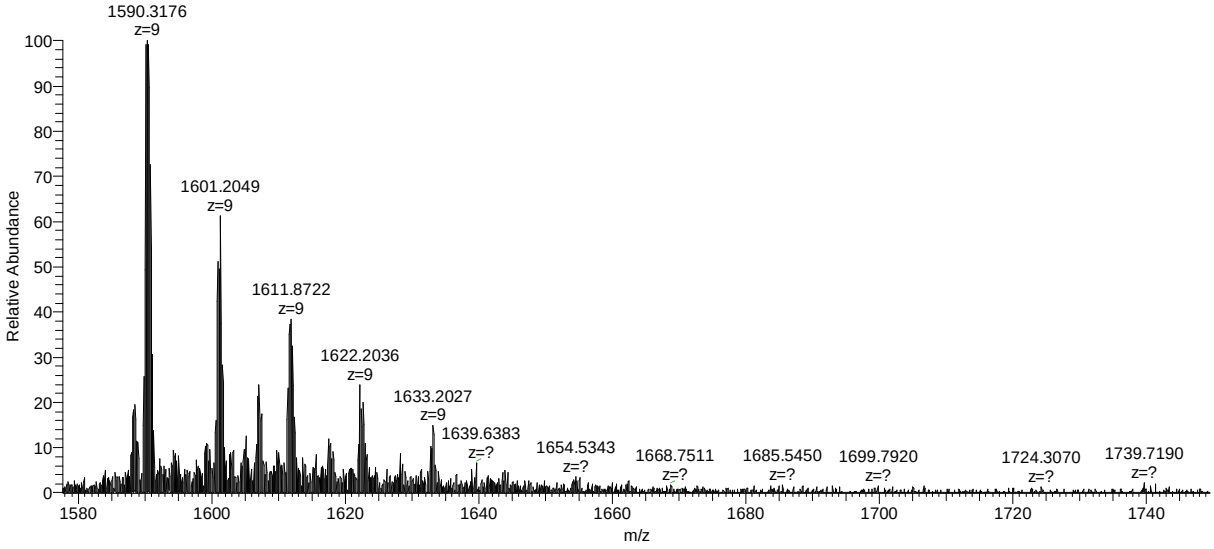

a)

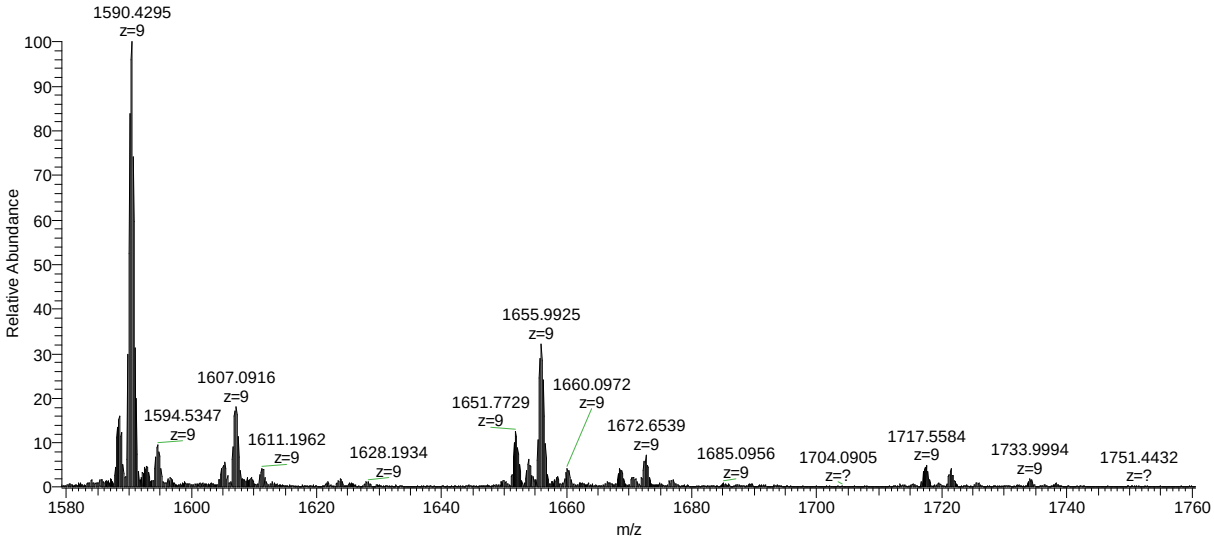

b)

Fig. S7 Original ESI MS mass spectra of lysozyme-adducts with Rh(III) complexes a) **1** and b) **2** in 1:1 (complex: HEWL) reaction ratio.

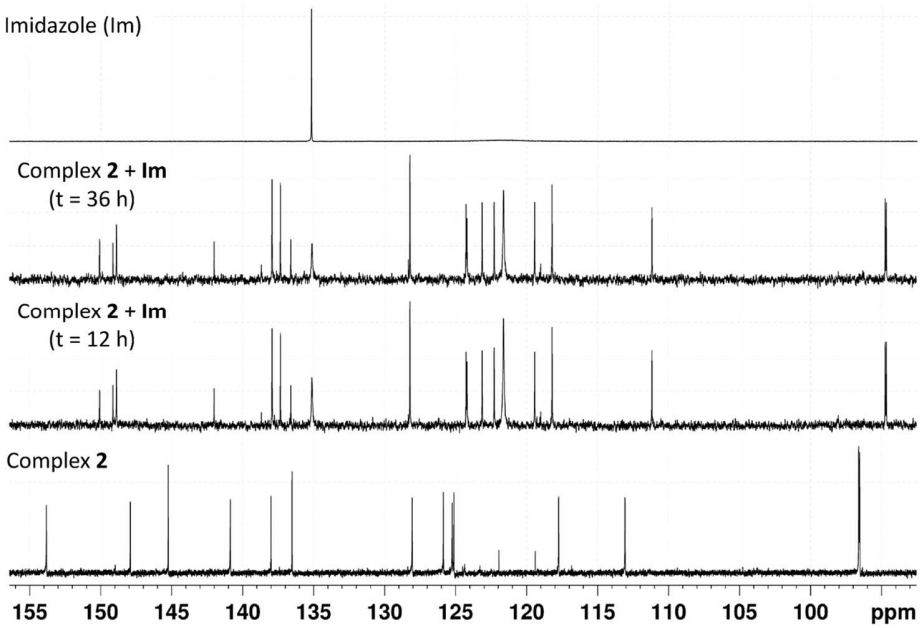

Fig. S8 ^{13}C NMR changes upon addition of imidazole to **2** in [D_6] DMSO.

Experimental Section

Materials and instruments

The chemicals, used in the synthesis of the benzimidazole ligands and their Rh(III) cyclopentadienyl compounds, were obtained from the commercial sources and used as received. 1-[(pyridin-2-yl)benzimidazole]-propyl-sulfonic acid (L^{SO3H}) [1], 1-ethyl-2-(pyridine-2-yl)benzimidazole (L^{ET}) [2], and 1,1'-(Hexane-1,6-diyl)bis[2-(pyridin-2-yl)1H-benzimidazole] (L^{BBZ}) [3], $[\{(\eta^5\text{-}C_5Me_5)RhCl\}_2(\mu\text{-}Cl)_2]$ [4] and 4,4,4-trifluoro-2-butynoic acid ethyl ester [5] were prepared by following the published approaches. Elemental (C, H, N and S) compositions of ligands and their complexes were obtained experimentally by Elementar Vario MICRO cube CHN analyzernor an EA 3000 elemental analyser from HEKtech. Solid-state infrared spectra were recorded on a Nicolet 380 FT-IR spectrometer. The {^{1}H, ^{13}C, ^{19}F and ^{31}P} NMR spectra were recorded with Bruker-Avance 500 (^{1}H, 500.13 MHz; ^{13}C{^{1}H}, 125.77 MHz; ^{19}F, 470.6 MHz; ^{31}P, 202.46 MHz) spectrometer. Two-dimensional NMR spectra ({^{1}H, ^{1}H} COS90 and {^{1}H, ^{13}C} HSQC) were recorded to precisely assign the resonances of NMR signals. Electrospray ionization mass spectrometry measurements were performed on ThermoFisher Exactive Plus instrument with an Orbitrap mass analyser at a resolution of R = 70.000 and a solvent flow rate of 5 µL min^{-1}. Electronic absorption spectra were recorded on a Specord 210 Plus spectrophotometer.

Synthesis of Rh(III) complexes

*Synthesis of $[RhCl(\eta^5\text{-}C_5Me_5)L^{ET}](CF_3SO_3)$ (**1**)*

To a beaker charged with $[\{(\eta^5\text{-}C_5Me_5)RhCl\}_2(\mu\text{-}Cl)_2]$ (124 mg, 0.2 mmol) and acetone (15 mL), was added $Ag(CF_3SO_3)$ (103 mg, 0.4 mmol). The reaction mixture was stirred for about one hour. Silver chloride was filtered off through Celite. The resulting clear red solution was then evaporated to dryness under vacuum. Red precipitate was re-dissolved in 1:1 (CH_3OH/CH_2Cl_2) mixture (15 mL) containing the ligand (L^{ET}) (178 mg, 0.8 mmol) and then the reaction mixture was stirred at 55 ^{o}C for 4 h. The volume of the resulting solution was decreased to about 7 mL, before adding diethyl ether (10 mL). The reaction mixture was left overnight, upon which red crystals formed, which were collected, washed with

diethyl ether, and dried under vacuum for four days. Yield: 61 % (160 mg, 0.25 mmol). IR (ATR, diamond): *v* = 2989 (w, CH), 1606 (m, CC/CN), 1492, 1435, 1265, 1138, 1031, 766 cm^{-1}. ^{1}H NMR (DMSO-d_6, 500.13 MHz): δ = 9.16 (dd, $^{3}J_{H,H}$ = 5.5 Hz, $^{4}J_{H,H}$ = 0.9 Hz, 1H, py-H6), 8.54 (d, $^{3}J_{H,H}$ = 8.6 Hz, 1H, py-H3), 8.41 (td, $^{3}J_{H,H}$ = 7.9 Hz, $^{4}J_{H,H}$ = 2.1 Hz, 1H, py-H4), 8.06 (dd, $^{3}J_{H,H}$ = 7.1 Hz, $^{4}J_{H,H}$ = 1.6 Hz, 1H, bim-H4), 7.94 (m, 1H, py-H5), 7.85 (m, 1H, bim-H7), 7.63 (m, 2H, bim-H5/H6), 4.94–4.86 (m, 2H, C*H*$_2$), 1.70 (s, 15H, Cp*–*CH*$_3$), 1.51 (t, $^{3}J_{H,H}$ = 7.2 Hz, 3H, CH_3) ppm. ^{13}C NMR (DMSO-d_6, 125.75 MHz): δ = 153.9 (py-C6), 147.7 (py-C2), 145.2 (bim-C2), 140.9 (py-C4), 138.1 (bim-C3a), 136.1 (bim-C7a), 128.0 (py-C5), 125.9 (bim-H5), 125.2 (bim-H6), 124.6 (py-C3), 120.6 (q, $^{1}J_{C-F}$ = 323 Hz, $CF_3SO_3^-$), 117.8 (bim-C7), 112.8 (bim-C4), 96.6 (d, $^{1}J_{C-Rh}$ = 8.0 Hz, Cp*–*C*CH_3), 40.7 (*C*H_2), 14.7 (*C*H_3), 9.1 (Cp*–CCH_3) ppm. ^{19}F NMR (DMSO-d_6, 470.6 MHz): δ = –77.7 ($CF_3SO_3^-$) ppm. ESI–MS (positive mode, acetone): 496.1042 {[RhCl(η^5-C_5Me_5)L^{ET}]}$^+$. $C_{25}H_{28}ClF_3N_3O_3RhS$: C 46.49, H 4.37, N 6.51, S 4.96; found C 46.59, H 4.36, N 6.77, S 4.66.

Synthesis of [RhCl(η^5-C_5Me_5)L^{SO3H}](CF_3SO_3*) (**2**)*

Preparation as for **1** with the ligand L^{SO3H} (203 mg, 0.8 mmol). The solvent mixture (CH_3OH/CH_2Cl_2) was removed under vacuum and the resulting red oily layer was re-dissolved by adding acetonitrile (20 mL). Filtration was done to remove the unreacted water-soluble ligand. Addition of diethyl ether (40 mL) to the filtrate yielded red precipitate. The precipitate was filtered off, washed with diethyl ether, and dried under vacuum. Yield: 38 % (80 mg, 0.11 mmol). IR (ATR, diamond): v = 3465 (br), 2924 (w, CH), 1603 (m, CC/CN), 1485 (m), 1457 (m), 1257 (s), 1156 (vs), 1029 (vs), 751 (s) cm^{-1}. ^{1}H NMR (DMSO-d_6, 500.13 MHz): δ = 9.15 (dd, $^{3}J_{H,H}$ = 5.4 Hz, $^{4}J_{H,H}$ = 1.1 Hz, 1H, py-H6), 8.89 (d, $^{3}J_{H,H}$ = 8.5 Hz, 1H, py-H3), 8.35 (td, $^{3}J_{H,H}$ = 8.1 Hz, $^{4}J_{H,H}$ = 1.5 Hz, 1H, py-H4), 8.13 (dd, $^{3}J_{H,H}$ = 7.2 Hz, $^{4}J_{H,H}$ = 1.5 Hz, 1H, bim-H4), 7.93 (m, 1H, py-H5), 7.83 (m, 1H, bim-H7), 7.62 (m, 2H, bim-H5/H6), 5.11–4.97 (m, 2H, NC*H*$_2$), 2.68 (m, 2H, C*H*$_2SO_3^-$), 2.18 (m, 2H, CH_2*CH*$_2CH_2$), 1.69 (s, 15H, Cp*–*CH*$_3$) ppm. ^{13}C NMR (DMSO-d_6, 125.75 MHz): δ = 153.8 (py-C6), 147.9 (py-C2), 145.2 (bim-C2), 140.9 (py-C4), 138.0 (bim-C3a), 136.5 (bim-C7a), 128.0 (py-C5), 125.9 (bim-H5), 125.2 (bim-H6), 125.1 (py-C3), 120.7 (q, $^{1}J_{C-F}$ = 321 Hz, $CF_3SO_3^-$), 117.8 (bim-C7),

113.1 (bim-C4), 96.6 (d, $^{1}J_{C-Rh}$ = 7.9 Hz, Cp*–*C*CH_3), 47.6 (C*H*$_2SO_3^-$), 44.45 (NC*H*$_2$), 25.6 (CH_2*CH*$_2CH_2$), 9.0 (Cp*–CCH_3) ppm. ^{19}F NMR (DMSO-d_6, 470.6 MHz): δ = –77.7 ($CF_3SO_3^-$) ppm. ESI-MS (positive mode, acetone): 612.0554 {Na[RhCl(η^5-C_5Me_5)L^{SO3H}]-H}$^+$, 590.0736 {[RhCl(η^5-C_5Me_5)L^{SO3H}]}$^+$, 554.0973 {{[Rh(η^5-C_5Me_5)L^{SO3H}]}$^+$. $C_{26}H_{30}ClF_3N_3O_6RhS_2$ ·0.5$C_4H_{10}O$, C 43.28, H 4.54, N 5.41, S 8.25, found, C 42.99, H 4.81, N 5.89, S 7.79.

X-ray crystallographic analysis

Red single-crystals suitable for X-ray crystallographic analysis were obtained by diffusion of diethyl ether into the solutions of **1** and **2** in 1:1 dichloromethane/methanol. The crystals were immersed in a film of perfluoropolyether oil, mounted on MiTeGen sample holders and relocated to a stream of cold nitrogen of the diffractometer. The crystallographic data was collected on a Bruker D8 QUEST diffractometer with a CMOS area detector and multi-layer mirror mono-chromated *Mo-K*$_\alpha$ radiation (λ = 0.71073 Å) at 100 K. All the diffracted intensities were corrected for Lorentz-polarization and absorption using the Bruker AXS software. The structures were solved with the SHELXT program using intrinsic phasing method [6] and refined with a full-matrix least-squares procedure using the SHELXL program [7] and expanded using Fourier techniques. All the non-hydrogen atoms were refined anisotropically refined. Hydrogen atoms were included in the structure factors calculations. All hydrogen atoms were assigned to idealized geometric positions. All lighter atoms in minor disorder part of main molecule were refined isotropic using a common scale. This U_{iso} value was estimated using a free variable and ADP similarity restraint to the major component of disorder (Residues 1--3 and 4). After that, the SIMU restraint was removed and constrained U_{iso} value was used for the final refinement cycle. Though residual values of the structure refinement of **2** were high, the structure solution could be considered as proof of the conformation of the molecule and metal to ligand ratio. Crystallographic data have been deposited with the Cambridge Crystallographic Data Centre as supplementary publication no. CCDC. 2024458 for compound **1**. These data can be obtained free of charge from The Cambridge Crystallographic Data Centre *via* www.ccdc.cam.ac.uk/data_request/cif.

Data	**1**
Empirical formula	$C_{25}H_{28}ClF_3N_3O_3RhS$
Formula weight ($g \cdot mol^{-1}$)	645.92
Temperature (K)	100(2)
Radiation, λ (Å)	$Mo_{K\alpha}$0.71073
Crystal system	Monoclinic
Space group	$P2_1/c$
Unit cell dimensions	
a (Å)	17.385(6)
b (Å)	9.6103(17)
c (Å)	17.425(7)
α (°)	90
β (°)	115.530(11)
γ (°)	90
Volume ($Å^3$)	2627.1(14)
Z	4
Calculated density ($Mg \cdot m^{-3}$)	1.633
Absorbtion coefficient (mm^{-1})	0.886
F(000)	1312
Theta range for collection	2.345 to 26.732°
Reflections collected	36849
Independent reflections	5561
Minimum/maximum transmission	0.6388/0.7456
Refinement method	Full-matrix least-squares on F^2
Data / parameters / restraints	5561 / 405 / 324
Goodness-of-fit on F^2	1.088
Final R indices [I>2σ(I)]	R_1 = 0.0416, wR^2 = 0.0890
R indices (all data)	R_1 = 0.0488, wR^2 = 0.0934
Maximum/minimum residual electron density ($e \cdot Å^{-3}$)	2.017 / –0.786

Lysozyme affinity of the complexes

Rh(III) compounds were dissolved in DMSO and then mixed with an equivalent quantity of the aqueous solution of HEWL to have a final solvent ratio of 20% (v/v) DMSO. A small volume of methanol was added to the aqueous mixture of **2**/HEWL of to be able to record the mass spectrum (20% (v/v) methanol). The mixtures were subsequently injected into the mass spectrometer to record the positive mode mass spectra. The spectra were recorded by direct introduction of the sample at a flow rate of 10 µL min^{-1}. The working conditions were as follows: spray voltage 3.80 KV, capillary voltage 45 V, and capillary temperature 320 ºC. For acquisition, Thermo Xaclibur qual was used.

Interaction of complex 2 with imidazole

The reaction between complex **2** and imidazole (Im) was investigated by ^{1}H and ^{13}C NMR in DMSO-d_6 at 298 K over 4 days using Brucker-Avance 400 (^{1}H: 400.40 MHz, and $^{13}C\{^{1}H\}$: 100.70 MHz) spectrometer. First, complex 2 was dissolved in DMSO-d_6 and NMR spectra were recorded. To NMR tube charged with complex **2**, imidazole was added and then the NMR spectra were recorded again.

Stability of the complexes

In control experiments, the stability of Rh(III) complexes in DMSO-d_6 as investigated by ^{1}H NMR analysis using Bruker-Avance 400 (^{1}H, 400.40 MHz) over 72 h (see Figure S5 for further details). In addition, UV-Vis absorption spectra of **1** (in 20% (v/v) DMSO/PBS) and **2** (in PBS and 20% (v/v) MeOH/PBS) as function of time were recorded over 48 h on a Specord 210 Plus spectrophotometer at 25 °C (PBS; 10 mM sodium phosphate buffer at pH 7.4). Other experimental settings were as follows: wavelength range: 240–900 nm, scan-time:600 nm/min, band width: 2.0 nm, data pitch: 1.0 nm

Biological activity testing

Antimicrobial screening was carried out by CO-ADD (The Community for Antimicrobial Drug Discovery), funded by the Wellcome Trust (UK) and The University of Queensland (Australia). No animals were used in this work. Cell lines (bacteria, fungi, and mammalian) were obtained from the American Type Culture Collection (ATCC). Human blood was obtained from the Australian Red Cross Blood Service with informed consent and its use in haemolysis assays was approved by The University of Queensland Institutional Human Research Ethics Committee, Approval Number 2014000031. The antimicrobial activity against seven fungi and bacteria, the cytotoxicity and haemolysis assays were evaluated at 32 μg/mL according to the protocols given elsewhere [8]. For toxic compound, a follow-up hit confirmation is triggered, where the toxicity is established by means of a dose-response assay against the same microbe strain.

Evaluation of antimicrobial activity

The antimicrobial activities of the synthesized ligands and their Rh(III) complexes were evaluated against cultures of *Staphylococcus aureus* ATCC 43300, *Escherichia coli* ATCC 25922, *Klebsiella pneumoniae* ATCC 700603, *Acinetobacter baumannii* ATCC 19606, *Pseudomonas aeruginosa* ATCC 27853, as well as two fungi, *Candida albicans* ATCC 90028 and *Cryptococcus neoformans var. grubii* H99; ATCC 208821. The samples were prepared in DMSO to a final testing concentration of 32 μg/mL and serially diluted 1:2 fold for 8 times. Each concentration was prepared in 384-well plates, non-binding surface plate (NBS; Corning 3640) for each bacterial/fungal strain, all in duplicate (n=2), and keeping the final DMSO concentration to a maximum of 0.5%. All bacteria were cultured in Cation-adjusted Mueller Hinton broth at 37 °C overnight. A sample of each culture was then diluted 40-fold in fresh broth and incubated at 37 °C for 1.5-3 h. The resultant mid-log phase cultures were diluted (CFU/mL, measured the absorbance at 600 nm), then added to each well of the compound containing plates, giving a cell density of 5×10^5 CFU/mL and a total volume of 50 μL. All the plates were covered and incubated at 37 °C for 18 h without shaking. The inhibition of the bacterial growth was determined by OD_{600} using a Tecan M1000 Pro monochromator plate reader. The percentage of growth inhibition was calculated for each well, using the negative control (media only) and positive control (bacteria

without inhibitors) on the same plate as references. The MIC was determined as the lowest concentration at which the growth was fully inhibited, defined by an inhibition ≥ 80%. In addition, the maximal percentage of growth inhibition is reported as D_{Max}, indicating any compounds with partial activity plates.

Fungi strains were cultured for 3 days on Yeast Extract-peptone Dextrose agar at 30 °C. A yeast suspension of 1×10^6 to 5×10^6 CFU/mL (determined by OD_{600}) was prepared from five colonies. The suspension was subsequently diluted and added to each well of the sample-containing plates giving a cell density of fungi suspension of 2.5×10^3 CFU/mL and total volume of 50 µL. All plates were covered and incubated at 35 °C for 36 h without shaking. The growth inhibition of *Candida albicans* was measured at 630 nm, while that of *Cryptococcus neoformans* was determined by measuring the difference in absorbance at 600 and 570 nm, after the addition of resazurin (0.001%, final concentration) and incubation at 35 °C for 2 h. The absorbance was measured using a Biotek Multiflo Synergy HTX plate reader and controls. The MIC was determined as the lowest concentration at which the growth was fully inhibited, defined by an inhibition = 80% for *Candida albicans* and an inhibition = 70% for *Cryptococcus neoformans*. Due to a higher variance in the growth and inhibition, a lower threshold was applied to the data for *Cryptococcus neoformans*. In addition, the maximal percentage of growth inhibition is reported as D_{Max}, indicating any compounds with marginal activity.

Cell viability Assay

Human embryonic kidney HEK293 cells were counted manually in a Neubauer haemocytometer and then plated in the 384-well plates containing the compounds to give a density of 5000 cells/well in a final volume of 50 µL. Dulbecco's Modified Eagle Medium (DMEM) supplemented with 10% FBS was used as growth media and the cells were incubated together with the compounds for 20 h at 37 °C in 5% CO_2. Cytotoxicity (or cell viability) was measured by Fluorescence (excitation 560/10, emission 590/10 nm) ($F_{560/590}$), after addition of 5 µL of 25 µg/mL resazurin (2.3 µg/mL final concentration) and after incubation for further 3 h at 37 37 °C in 5% CO_2. The intensity was measured using Tecan M1000 Pro monochromator plate reader,

using automatic gain calculation. CC_{50} (the concentration at 50% cytotoxicity) was calculated by curve fitting the inhibition values *vs.* logC using a sigmoidal dose-response function, with variable fitting values for bottom, top and slope. The curve fitting was implemented using Pipeline Pilot's dose-response component, resulting in similar values to curve fitting tools such as GraphPad's Prism and IDBS's XlFit.

References

1 A.M. Mansour, O.R. Shehab, *Dalton Trans.* 2018, **47**, 3459.

2 A.M. Mansour, O.R. Shehab, K. Radacki, *Eur. J. Inorg. Chem.* 2020, 299.

3 A.M. Mansour, A. Friedrich, *New J. Chem.* 2018, **42**, 18418.

4 C. White, A. Yates, P. M. Maitlis, D. M. Heinekey, *Inorg. Synth.* 1992, **29**, 228.

5 B.C. Hamper, *Org. Synth.*, 1992, **70**, 246.

6 G. M. Sheldrick, *Acta Crystallogr.*, 2015, **A71**, 3.

7 G. M. Sheldrick, 2008, **A64**, 112.

8 A. Frei, J. Zuegg, A.G. Elliott, M. Baker, S. Braese, C. Brown, F. Chen, C.G. Dowson, G. Dujardin, N. Jung, A.P. King, A.M. Mansour, M. Massi, J. Moat, H.A. Mohamed, A.K. Renfrew, P.J. Rutledge, P.J. Sadler, M.W. Todd, C.E. Willans, J.J. Wilson, M.A. Cooper and M.A.T. Blaskovich, *Chem. Sci.* 2020, **11**, 2627.